

AMPEROMETRIC MICROSENSORS FOR SCREENING OF PROTEIN FRACTIONS FOR ENZYMATIC ACTIVITIES

S. Pavoni^{a}, C. Sundermeier^b, J. Perdomo^c, H. Hinkers^b*

^aCentro de Investigaciones en Microelectrónica (CIME/ISPJAE) PO BOX 8016, Havana 8, Cuba

^bInstitut für Chemo- und Biosensorik (ICB), Mendelstraße 7, D-48149 Münster, Germany

^cUniversidad de las Ciencias Informáticas (UCI), Havana, Cuba

*E-mail-address: pavoni@uni-muenster.de

ABSTRACT

In this paper we report on the development of amperometric sensors containing micro- and macro electrodes which are fabricated in thin film technology. A comparison of the most important parameters like sensitivities and response times is made with respect to their potential application fields in protein screening experiments. Chips fabricated with different substrate materials are compared and also chips with different electrode materials. As a result the macro electrodes exhibit some important advantages over the micro electrodes in this application field and the conventional Ag/AgCl reference electrode may be replaced by a platinum electrode for stability reasons.

1. INTRODUCTION

The systematic genome-sequencing programs revealed a lot of genes whose functions are still unknown. A possible approach to get insight in the functions is via the protein identification. This can be done by 2dim electrophoresis. But this method is restricted to proteins smaller than 100 kDa. Also MALDI-MS (matrix-assisted laser desorption/ionisation mass spectroscopy) is used to identify catalytically active proteins (enzymes). But this method is restricted to enzymes catalyzing reactions whose products are larger than about 300 Da. The detection of such products with amperometric detection principles may, thus, be a promising method complementary to MALDI-MS. However, the sensors must be fast and small, since there are often only very small amounts of analyte solution available and the analyte consumption by the sensor must be kept low. In this paper we report on the development of appropriate sensors containing micro- and macro electrodes which are fabricated in thin film technology.

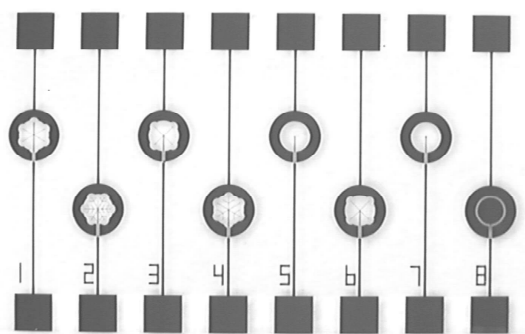


Fig. 1. Photo of the chip containing sensors with eight different electrode geometries.

Since the diffusion field of an ultra-microelectrode is spherical rather than planar, a nearly steady-state current may be obtained even in a nearly quiescent solution [1,2]. A fast current response to changes of the applied potential is also expected. However, because of their extremely small size the current output in microelectrodes is very low. Higher current signals can be achieved by the use of arrays of electrodes. The distance between the single electrodes is an important parameter which has to be optimized properly. Therefore test chips have been developed containing eight different electrode geometries [3].

2. RESULTS AND DISCUSSION

The sensors were fabricated in a two-electrode configuration with a pseudo reference electrode and a working electrode resp. an array of working electrodes with different sizes and geometrical arrangements. In fig. 1 a photo of the chip is shown. The diameters and the

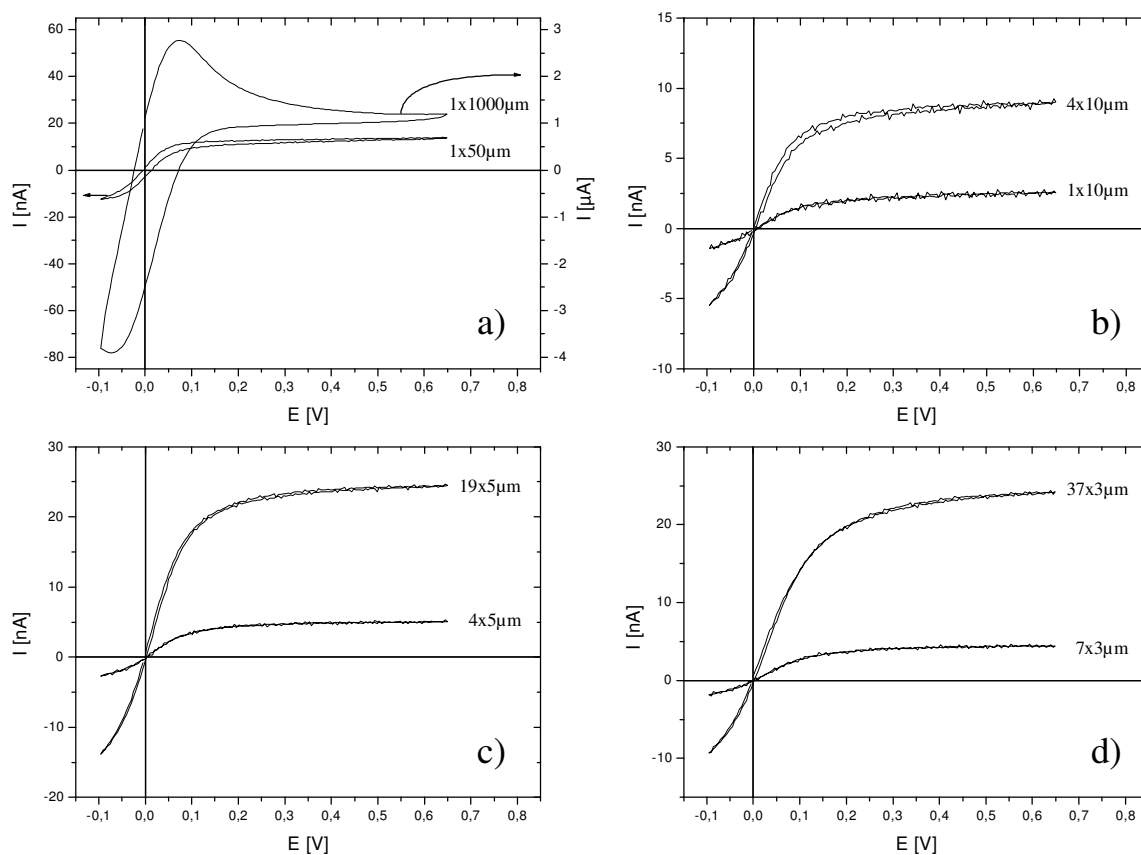


Fig. 2. Cyclic voltammograms using a solution of 2,5mM $K_3[Fe(CN)_6]$ and 2,5mM $K_4[Fe(CN)_6]$ in 0,1M KCl. The measurements were made with one of the silicon chips containing platinum pseudo reference electrodes.

number of the working electrodes per array were: 1x1000µm (macro electrode), 1x50µm, 4x10µm, 1x10µm, 19x5µm, 4x5µm, 37x3µm, and 7x3µm. The working electrodes were made of Pt. The pseudo reference electrode consists of a ring of Pt resp. Ag/AgCl with an active area of about 2mm² surrounding the array of working electrodes. The working electrode is located in the centre of the surrounding reference electrode or - in the case of the arrays - the single electrodes are equally distributed within a circular area of 1mm diameter.

The chips were fabricated with thin-film technologies on oxidized Si wafers (1 µm SiO₂) and in comparison on glass wafers both with 3" diameters. The fabrication process consisted of three photolithographic steps. In a first step the Pt layer was structured in a lift-off process. The Pt layer of 120 nm was sputter deposited together with an adhesion layer of Ti of 40 nm. A sacrificial layer of Al (evaporated in a PVD process) was used for the lift-off-process. In a second lithographic process the insulation layer of 260nm of Si₃N₄ was patterned defining the active electrode areas. Finally, an OTS (C₁₃-Si-

((CH₂)₁₇-CH₃) coating was deposited to obtain a hydrophobic sensor surface. This layer was patterned in a third lithographic process to define hydrophilic surfaces in the region of the electrodes. Additionally, some chips got a silver layer on top of the pseudo reference electrodes. These electrodes were chloridized using 0,2M of FeCl₃ to get a AgCl surface.

The response of the electrodes was first tested with cyclic voltammetry (CV) using a solution of 2,5mM $K_3[Fe(CN)_6]$ and 2,5mM $K_4[Fe(CN)_6]$ in 0,1M KCl. The measurements were made with one of the silicon chips containing platinum pseudo reference electrodes. The potential was scanned from +0,65V to -0,1V with a scan rate of 500mV/s. A drop of 10 µl of the analyte solution was deposited onto the surface of the electrodes. The surrounding OTS layer served as a hydrophobic barrier resulting in a very well defined and reproducible shape of the drops. The results are shown in fig. 2 a-d. First, fig. 2a shows the typical peak-shaped voltammogram of a macro electrode where mass transport is dominated by

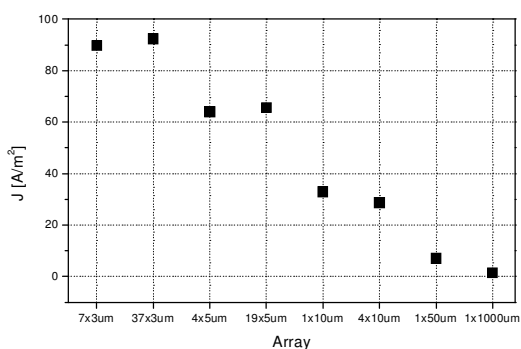


Fig. 3. Steady state current densities of the 8 different electrode configurations. The current densities have been calculated from the current values in fig. 2 at $E=0.65\text{V}$ divided by the total electrode area.

linear diffusion. Also in fig. 2a the voltammogram of the 50um electrode is shown. It clearly shows the change from the peak-shaped voltammogram to a sigmoidal voltammogram reflecting the change from linear to radial diffusion. At even smaller electrode diameters (fig. 2 b-d) the voltammograms are dominated by pure radial diffusion. It is interesting to notice that the shape of the voltammograms is roughly independent of the number of electrodes forming the sensor array - at least at the smallest diameters of 5um and 3um (fig. 2c, d). This means that the single electrode distances are large enough to prevent overlaps of the diffusion fields of the neighboring electrodes. The total current of the array of working electrodes is then proportional to the number of single electrodes. This is demonstrated in fig. 3 where the steady state current densities of the 8 different electrode configurations are compared. The current densities have been calculated from the current values in fig. 2 at $E=0.65\text{V}$ divided by the total electrode area. As expected the highest current densities of around $90\mu\text{A}/\text{mm}^2$ were achieved with the 3um electrodes followed by $65\mu\text{A}/\text{mm}^2$ for the 5um electrode and ending with $1,5\mu\text{A}/\text{mm}^2$ for the macro electrode.

Next, the calibration curves and the sensitivities were determined for the different electrode geometries. Many different kinds of the technically and medically relevant enzymes may produce hydrogen peroxide - either directly as an end product of the catalytic pathway or by the inclusion of additional reaction steps. Therefore, the determination of the sensitivities and the calibration curves was performed with hydrogen peroxide. A 66,7mM potassium phosphate buffer solution with 138mM NaCl and $\text{pH}=7,2$ was used and different amounts of H_2O_2 were added to achieve concentrations between 10uM and 40mM). In fig. 4 the calibration curve

of the macro electrode is compared with those of the micro electrodes. The measurements have been performed with a silicon chip and the polarization potential was +800mV via the integrated Pt pseudo-reference electrode. The linear range of the macro electrode exceeded 40mM whereas those of the micro electrodes were found in the range between 20mM and 30mM (this is valid also for the electrodes not shown in fig. 4.) The macro electrode revealed by far the highest sensitivity of $202\text{nA}/\text{mM}$ followed by $7,0\text{nA}/\text{mM}$ of the 50um electrode (not shown in fig. 4). The micro electrodes revealed sensitivities of $1,6\text{nA}/\text{mM}$ (4x10um), $1,3\text{nA}/\text{mM}$ (19x5um), and $1,4\text{nA}/\text{mM}$ (37x3um).

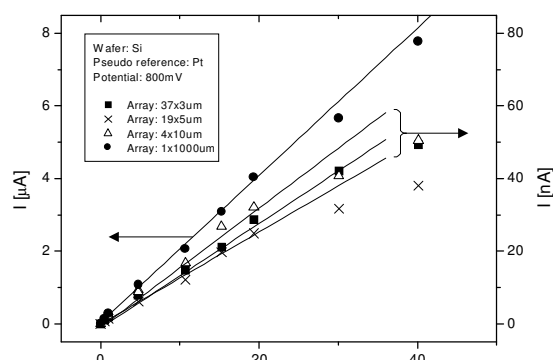


Fig. 4. Calibration curves for different electrode geometries. A 66,7mM potassium phosphate buffer solution with 138mM NaCl and $\text{pH}=7,2$ was used and different amounts of H_2O_2 were added to achieve concentrations between 10uM and 40mM).

Next we checked the response of the sensor signals on voltage switching. The sensor was equipped with a buffer solution containing $500\mu\text{M}$ H_2O_2 . Then the potential of +800mV was switched on. This resulted in a peak-shaped response curve as shown in fig. 5a. The maximum peak current was followed by a decrease until a quasi steady state current I_{final} was reached. A detailed analysis of the complex response behavior would need to include several parameters and effects like depletion layer capacity, chip capacities, chemical composition of the electrode surfaces, build up of the diffusion layer, evaporation of the solution, analyte consumption, and others. This theoretical treatment has been omitted in this paper. But the response times have been determined experimentally for the different sensors. The response times were defined as follows: t_5 is the time from the voltage switching until a current value of $1,05 \cdot I_{\text{final}}$ is reached. Similarly t_{10} is the time until $1,10 \cdot I_{\text{final}}$ is reached. The definitions are explained in fig. 5a. The results are shown in fig. 5b.

They were obtained using a silicon based sensor chip which was again equipped with Pt pseudo reference electrodes. If the response times were dominated by

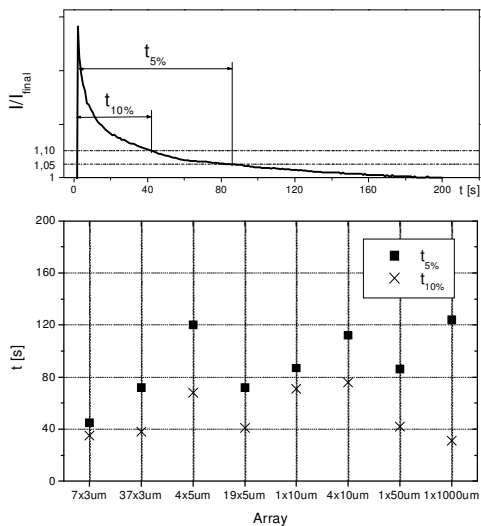


Fig. 5. a) Response time definition: t_5 is the time from the voltage switching until a current value of $1.05 \cdot I_{final}$ is reached and t_{10} is the time until $1.10 \cdot I_{final}$ is reached. b) Response time of the different electrode geometries.

depletion layer effects one would expect increasing response times with increasing electrode diameters. This is obviously not the case. The t_5 times are distributed between about 40s and 120s tending to higher values with increasing electrode diameters. But the t_{10} times seem to be randomly distributed between about 35s and 80s. The shape of the response curves of the micro electrodes is very similar to the one shown in fig. 5a exhibiting a continuously decreasing current. On the other hand the macro electrode shows a different behavior with a minimum in the $I(t)$ -curve followed by a flat maximum until I_{final} is reached (fig. 6). This behavior results in a rather short t_{10} time for the macro electrode. Interestingly it is the shortest t_{10} time of all the electrodes investigated here. Having the great advantage of the huge sensitivity in mind the macro electrode was therefore chosen as the primary candidate for the further investigations.

It was also checked whether the different substrate materials of the chips (glass or silicon) or the different materials of the pseudo reference electrodes (Pt or AgCl) would influence the response characteristics or the sensitivity of the sensors. First in fig.6 a glass chip was

compared with a silicon chip both equipped with Ag/AgCl-reference electrodes. The experiment to determine the response functions was carried out in a slightly different way from the one described above: The chip was first equipped with the pure buffer solution and the voltage was then switched on. After 3min the measurement was started ($t=0$ in fig. 6). Then at $t=100$ s

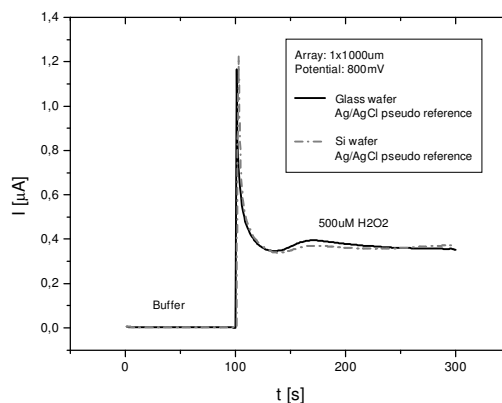


Fig. 6. Response functions of a glass chip compared with silicon chip, both equipped with Ag/AgCl-reference electrodes.

the buffer solution was removed and immediately replaced by a 500uM H_2O_2 solution. The sudden change of the analyte solution produced a current peak very similar to the one occurring on voltage switching. The resulting response curves in fig. 6 are very similar for the glass and silicon chips. This is especially true for the

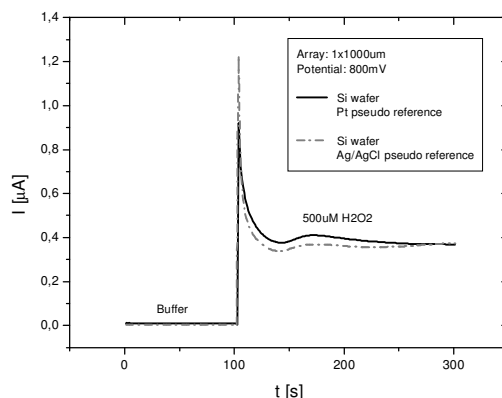


Fig. 7. Response functions of two chips fabricated in silicon, the first one equipped with a Pt and the second one with a Ag/AgCl pseudo reference electrode.

response times which are $t_5=17s$ and $t_{10}=14s$ for both chips. Thus, it seems to be clear that the chip capacities which should be very different for glass and silicon substrates do not contribute significantly to the response time of the sensor. Also - as expected - the sensitivities of the two sensors were practically identical. It is important to notice that the response times determined in this experiment much smaller than those observed in the previous one. Thus, the external voltage switching seems to produce a larger disturbance on the sensor signal compared with the change of the analyte solution. Perhaps the current is not completely interrupted during the analyte change although the sensor surface seems to be macroscopically dry.

In fig. 7 similar results are shown for two chips which are both fabricated in silicon, but the first one was equipped with a Pt and the second one with a Ag/AgCl pseudo reference electrode. Again, the response curves are very similar. But the response times are now different. The t_5 time for the Ag/AgCl electrode is 17s compared with 29s for the Pt electrode and the t_{10} times are 14s for the Ag/AgCl electrode resp. 23s for the Pt electrode. As a reason the double layer capacities may be different for the two electrodes or - in the case of the Pt electrode - it may take some time until the thermodynamical equilibrium is reached after the analyte change.

3. CONCLUSIONS AND OUTLOOK

Fast, sensitive, and longterm stable sensors are needed for future applications in enzyme screening. It has been demonstrated within this paper that platinum may be used as material not only for the working electrode but also for the pseudo reference electrode. This has some advantages over silver electrodes. First, the longterm stability of the thin film Ag/AgCl electrodes is often very limited. Furthermore, silver is known to be an efficient inhibitor of many enzymatic reactions. On the other hand platinum is very stable and compatible with the proteins and other biological species. Therefore, if the analysis time is not the limiting factor in protein screening tasks, platinum should be used as electrode material. It has also been demonstrated that macro electrodes may be used for protein screening purposes instead of micro electrodes. There was no great advantage of the micro electrodes over macro electrodes concerning response times of the sensors on voltage switching and analyte change. On the other hand the macro electrode is much more sensitive than the micro electrodes and the detection limit for the proteins may be reduced. As a further advantage the macro electrodes may also be fabricated in e.g. screen printing technology, which may have some cost advantages over thin film technologies. In a next step an

array of sensors will be set up, which will be compatible with the 96 well micro titre plate format. The simultaneous readout of complete columns of sensors will be performed using a multiplexing technique which has already been demonstrated previously [4].

Acknowledgement

S. Pavoni and J. Perdomo greatly acknowledge the financial support of the Deutsche Akademische Austauschdienst (DAAD).

4. REFERENCES

- [1] A.J. Bard, L.R. Faulkner, *Electrochemical Methods: Fundamentals and Applications*, John Wiley & Sons, New York, 1980.
- [2] K. Aoki, "Theory of Ultramicroelectrodes" *Electroanalysis* 5, pp. 627-639, 1993.
- [3] W. E. Morf, N. F. de Rooij, "Performance of amperometric sensors based on multiple microelectrode arrays" *Sensors and Actuators B* 44, pp. 538-541, 1997.
- [4] H. Hinkers, T. Hermes, C. Sundermeier, M. Borchardt, C. Dumschat, S. Bücher, M. Bühner, K. Cammann, M. Knoll, "An Amperometric Microsensor Array with 1024 Individually addressable Elements for Two dimensional Concentration Mapping", *Sensors & Actuators B* 24, pp. 300-303, 1995.